Most supermassive black hole growth is obscured by dust

Supplementary Information

Alejo Martínez-Sansigre[†], Steve Rawlings[†], Mark Lacy[‡], Dario Fadda[‡], Francine R. Marleau[‡], Chris Simpson[⋆], Chris J. Willott[⋄], Matt J. Jarvis[†]

[†]Astrophysics, Department of Physics, University of Oxford, Keble Road, Oxford OX1 3RH, UK
[‡]Spitzer Science Center, California Institute of Technology, MS220-6, 1200 E. California Boulevard, Pasadena, CA 91125, USA
[⋆]Department of Physics, University of Durham, South Road, Durham DH1 3LE, UK
[⋄]Herzberg Institute of Astrophysics, National Research Council, 5071 West Saanich Rd, Victoria, B.C. V9E 2E7, Canada

---

This document provides supplementary information for the above letter to Nature. We discuss further our selection criteria and our results for the quasar fraction.

Supplementary Notes

The mid-infrared criterion was chosen to select quasars below the "break" in the luminosity function at $z \sim 2$. The peak of the quasar activity occurred at this redshift and by targeting the quasars around the "break" we would be sensitive to the dominant part of the population. The $S_{24\mu\mathrm{m}} > 300$ μJy criterion was chosen to obtain a reliable (7-σ) catalogue from the Spitzer FLS data from the MIPS instrument [1] (Fadda, D., *et al.*, in preparation). At $z = 2$, this corresponds to an emitted 8-μm luminosity $L_{8\mu\mathrm{m}} = 10^{24.4}$ W Hz^{-1}. Assuming a typical Type-1 SED[2], this corresponds to $L_{\mathrm{B}} = 10^{23.2}$ W Hz^{-1} or $M_{\mathrm{B}} = -23.8$. At $z = 2$, the break in the quasar luminosity function, L^{*}_{quasar}, corresponds to $M_{\mathrm{B}} = -25.7$[3] (with Pure Luminosity Evolution[3]), so our 24-μm selection will select quasars $\gtrsim 0.2\ L^{*}_{quasar}$ at $z = 2$, and more luminous quasars at higher redshifts.

Quasars are normally considered as being Type-2 if they have an $A_{\rm V} \gtrsim 5$[4] which will make their observed near-infrared emission much fainter than that of Type-1s. The near-infrared criterion was therefore chosen to remove naked (Type-1) quasars as well as lower redshift ($z \lesssim 1.4$) Type-2s. At $z \geq 2$ the detected 3.6-μm flux density corresponds to light emitted at $\lambda \leq 1.2\ \mu$m so dust extinction ensures that Type-2 quasars are much fainter than Type-1 quasars, even for a moderate A_V. Indeed, the $S_{3.6\mu{\rm m}}$ emission is likely to be dominated by starlight for $A_V \geq 10$, and since light at 3.6-μm is dominated by the old stellar population, there will be an $S_{3.6\mu{\rm m}} - z$ correlation, analogous to the $K - z$ relation for radio galaxies[5]. A typical host galaxy for a $z = 2$ radio-quiet quasar has a luminosity of $2L^{*}_{gal}$[6], so we adapt the $K - z$ relation (which assumes $3L^{*}_{gal}$ hosts for radio galaxies[5]) to $2L^{*}_{gal}$ hosts at 3.6-μm (where L^{*}_{gal} is $M_{\rm K} = -24.28$, 2MASS Kron Magnitudes[7]). This criterion corresponds to a limiting 'photometric redshift' $z_{\rm phot} \gtrsim 1.4$. The scatter in true host luminosity means that individually, the photometric redshifts are not necessarily close to the spectroscopic redshift, but they agree on average (there is no obvious systematic $z_{\rm phot}$ error from the objects with spectroscopic redshift in Table 1 but there is clearly much scatter). Changing the host galaxy from an elliptical to a (non-starburst) spiral does not change the $z_{\rm phot}$ significantly. For the objects that have spectroscopy, the mean and median photo-zs are 2.75 and 2.65 respectively while the mean and median spectroscopic redshifts are 2.35 and 2.00: This represents good agreement for such a simple photometric redshift algorithm and gives us some confidence that we can estimate how many objects that remained unobserved or had blank optical spectra are at $z \geq 2$. A possible source of error for our photometric redshifts would be the contribution of quasar light to $S_{3.6\mu{\rm m}}$. From supplementary FIG. 1 we can see that although $S_{4.5\mu{\rm m}}$ might sometimes be significantly contaminated by quasar light, $S_{3.6\mu{\rm m}}$ is not.

The sample was selected from the preliminary 3.6 and 24 μm catalogues[1] (Fadda, D., *et al.*, in preparation, Lacy, M.,*et al.*, in press) but the flux densities quoted are the final ones. The 'parent' population plotted on FIG. 1 of the main letter have not yet had their flux densities re-measured. This explains why we have a source (ams19) with $S_{3.6\mu\mathrm{m}} = 45.2$ μJy in our sample when our 3.6 μm criterion was ≤ 45 μJy and another source (ams02) with $S_{24\mu\mathrm{m}}$ slightly below the flux density limit of 300 μJy. The preliminary 24 μm catalogue had a flux density limit of 300 μJy which explains why all the sources with $S_{24\mu\mathrm{m}} < 300$ μJy are plotted as upper limits.

The mean radio flux density of the sample is 782 μJy, which at the mean spectroscopic redshift $z = 2.38$ corresponds to a radio luminosity of $L_{1.4\ \mathrm{GHz}} = 2 \times 10^{24}$ W Hz^{-1} sr^{-1} (assuming a mean spectral index $\alpha = 0.8$). This is well below the break in the RLF[8] where typical radio-selected objects have Fanaroff-Riley Class I radio structures[9], little direct evidence of associated optical quasar activity[10] and weak or absent emission lines suggesting that, whether or not obscuring tori exist in this class of objects[11], any associated quasar is accreting at a very low rate[12]. Our objects differ from typical radio-selected objects in several respects: once the obscuration of the quasar nucleus is accounted for, they have the high accretion rates of typical quasars, but relatively low radio luminosities, and their radio structures appear compact rather than FRI. However, we caution[13] that there are complicated selection biases at work here.

To interpret our results in terms of the 'quasar fraction' q – the ratio of the number of Type-1 quasars to the total number of Type-1 and Type-2 quasars – we need to predict the average number $< N_1 >$ of Type-1 quasars meeting identical $S_{24\mu\mathrm{m}}$ and $S_{1.4\mathrm{GHz}}$ selection criteria, and having matched redshift and sky area selection functions. To account for the various uncertainties, we estimate a probability distribution p($< N_1 >$). The most important of these, and the dominant contributor to the width of p($< N_1 >$), results from the lower $S_{1.4\mathrm{GHz}}$ cut. This cut greatly reduces the number of quasars by excluding the low-luminosity end of the radio-quiet population[14]. We use the B-band luminosity function[15], adopt a radio luminosity versus optical luminosity correlation, including a measured scatter, for Type-1 quasars[16] and generate a probability distribution for the fraction of Type-1 quasars with $S_{24\mu m} > 300$ μJy and $z \geq 2$ which would fall in our target range in $S_{1.4\mathrm{GHz}}$. We assume a radio spectral index $\alpha = 0.80$ (where flux density $\propto \nu^{-\alpha}$) and estimate the possible range between $\alpha = 0.50$ and 1.00. For the conversion between observed 24-μm flux densities and restframe B-band luminosities, we assume a spectral index $\alpha = 1$ (where $L_\nu \propto \nu^{-\alpha}$) and vary the range between $\alpha = 0.85$ and 1.15[17]. We also assume pure luminosity evolution (as this allows us to predict exactly the number of Type-1 quasars of ref[18], which gives us confidence in our method) and quantify uncertainties by varying between pure luminosity evolution and pure density evolution[15]. All the errors are then combined in quadrature.

To obtain the normalised posterior probability $\mathrm{p}(q|\mathrm{data}, \{\mathrm{Type}-1\ \mathrm{quasar}\})$ we use Bayes' theorem with a uniform prior over the range $0 \leq q \leq 1$ so that the $\mathrm{p}(q|\mathrm{data}, \{\mathrm{Type}-1\ \mathrm{quasar}\}) = \mathrm{p}(\mathrm{data}|q, \{\mathrm{Type}-1\ \mathrm{quasar}\})$. We then calculate this likelihood function, at each q, as a Poisson distribution for the observed (integer) number of Type-2 quasars at $z \geq 2$ where the mean number expected $< N_2 >= (1-q) < N_1 > /q$. Note that Poisson sampling fluctuations are correctly excluded from the error budget because we are interested in $< N_1 >$ and not the patch-to-patch variance of N_1.

Finally, we compare our results with unified schemes[19] by considering models in which, for Type-2 objects, a dusty torus obscures direct view of the quasar nucleus. Our preferred value $q = 0.2 - 0.4$ (FIG. 2) implies a torus half-opening angle $\theta \approx 40°$ for $z \sim 2.5$ quasars. At first sight this does not sit easily with the 'receding torus' models[20,21] in which the solid angle subtended by the torus decreases, and hence q increases, systematically with increasing quasar luminosity. As our selection criteria select luminous quasars (FIG. 1), the torus should have receded to the point that $q \approx 0.6$. We suggest that the resolution of this problem is that there is increased kpc-scale dust obscuration affecting both the nuclear and narrow-line regions in some fraction of $z \sim 2$ quasars. This would explain why a good fraction of our optical spectra were completely blank. Thus, receding torus models should only be compared to the solid blue line (with $q \approx 0.4$) and perfectly consistent with the data. Similar spectroscopic studies of radio-loud Type-2 quasars[22] almost always yield narrow emission lines, presumably because extended radio sources clear dust and gas from the inner part of the host galaxy[23]. The properties we infer for our 'blank spectrum' Type-2 quasars are those predicted for obscured growing supermassive black holes[24,25].

References

[1] Marleau, F.R., *et al.*, Extragalactic Source Counts at 24 Microns in the Spitzer First Look Survey, *Astrophys. J. S.*, **154**, 66-69 (2004)

[2] Rowan-Robinson, M., A new model for the infrared emission of quasars, *Mon. Not. R. Astr. Soc.* **272**, 737-748 (1995)

[3] Croom, S.M., *et al.*, The 2dF QSO Redshift Survey-XII. The spectroscopic catalogue and luminosity function, *Mon. Not. R. Astr. Soc.* **349**, 1397-1418 (2004)

[4] Simpson, C., Rawlings, R., Lacy, M., Thermal-infrared imaging of 3C radio galaxies at z$\sim$1, *Mon. Not. R. astr. Soc.* **306**, 828-842 (1999)

[5] Willott, C.J., Rawlings, S., Jarvis, M.J., Blundell, K.M., Near-infrared imaging and the $K-z$ relation for radio galaxies in the 7C Redshift Survey, *Mon. Not. R. astr. Soc.* **339**, 173-188 (2003)

[6] Kukula, M.J., *et al.*, A NICMOS study of high-z quasar host galaxies, *Mon. Not. R. astr. Soc.* **326**, 1533-1546 (2001)

[7] Cole, S., *et al.*, The 2dF galaxy redshift survey: near-infrared galaxy luminosity functions, *Mon. Not. R. astr. Soc.* **326**, 255-273 (2001)

[8] Willott, C.J., Rawlings, S., Blundell, K.M., Lacy, M., The radio luminosity function of radio-loud quasars from the 7C Redshift Survey, *Mon. Not. R. astr. Soc.* **300**, 625-648 (1998)

[9] Fanaroff, B.L., Riley, J.M., The morphology of extragalactic radio sources of high and low luminosity, *Mon. Not. R. astr. Soc.* **167**, 31-36 (1974)

[10] Grimes, J.A., Rawlings, S., Willott, C.J., Implications for unified schemes from the quasar fraction and emission-line luminosities in radio-selected samples, *Mon. Not. R. astr. Soc.* **349**, 503-517 (2004)

[11] Chiaberge, M., Capetti, A., Celotti, A., The HST view of FR I radio galaxies: evidence for non-thermal nuclear sources, *Astron. Astrophys* **349**, 77-87 (1999)

[12] Rawlings, S., Saunders, R., Evidence for a common central-engine mechanism in all extragalactic radio sources, *Nature* **349**, 138-140 (1991)
[13] Blundell, K.M., Rawlings, S., The Optically Powerful Quasar E1821+643 is Associated with a 300 Kiloparsec-Scale FR I Radio Structure, *Astrophys. J.* **562**, 5-8 (2001)
[14] Jarvis, M.J., Rawlings, S., The accretion history of the universe with the SKA, *New Astronomy Reviews* **48**, 1173-1185 (2004)
[15] Wolf, C., *et al.*, The evolution of faint AGN between z$\sim$1 and z$\sim$5 from the COMBO-17 survey, *Astron. Astrophys* **408**, 499-514 (2003)
[16] Cirasuolo, M., Celotti, A., Magliocchetti, M., Danese, L. Is there a dichotomy in the radio loudness distribution of quasars? *Mon. Not. R. Astr. Soc.* **346**, 447-455 (2003)
[17] Neugebauer, G., *et al.*, Continuum energy distributions of quasars in the Palomar-Green survey, *Astrophys. J.S.* **63**, 615-644 (1979)
[18] Zheng, W., *et al.*, Photometric redshifts of X-ray sources in the Chandra Deep Field South, *Astrophys. J. S.* **155**, 73 (2004)
[19] Antonucci, R., Unified models for active galactic nuclei and quasars, *Ann.Rev.Astron.Astrophys.* **31**, 473-521 (1993)
[20] Lawrence, A., The relative frequency of broad-lined and narrow-lined active galactic nuclei – implications for unified schemes, *Mon. Not. R. Astr. Soc.* **252**, 586-592 (1991)
[21] Simpson, C., A new look at the isotropy of narrow-line emission in extragalactic radio sources, *Mon. Not. R. Astr. Soc.* **297**, L39-L43 (1998)
[22] Rawlings, S., Eales, S., Lacy, M., A sample of 6C radio sources with virtually complete redshifts-II.Optical spectroscopy, *Mon. Not. R. astr. Soc.* **322**, 523-535 (2001)
[23] Baker, J.C., *et al.* Associated absorption in radio quasars. I. C IV absorption and the growth of radio sources, *Astrophys. J.* **568**, 592-609 (2002)
[24] Fabian, A.C., The obscured growth of massive black holes, *Mon. Not. R. Astr. Soc.* **308**, L39-L43 (1999)
[25] Alexander, D.M., *et al.*, Rapid Growth of Black Holes in Massive Star-Forming Galaxies, *Nature* **434**, 738-740 (2005)
[26] Bruzual, G., Charlot, S., Stellar population synthesis at the resolution

of 2003, *Mon. Not. R. Astr. Soc.* **344**, 1000-1028 (2003)
[27] Sajina, A., *et al.*, The 2-850 micron SED of starforming galaxies, astro-ph/0412394

Supplementary Figure 1

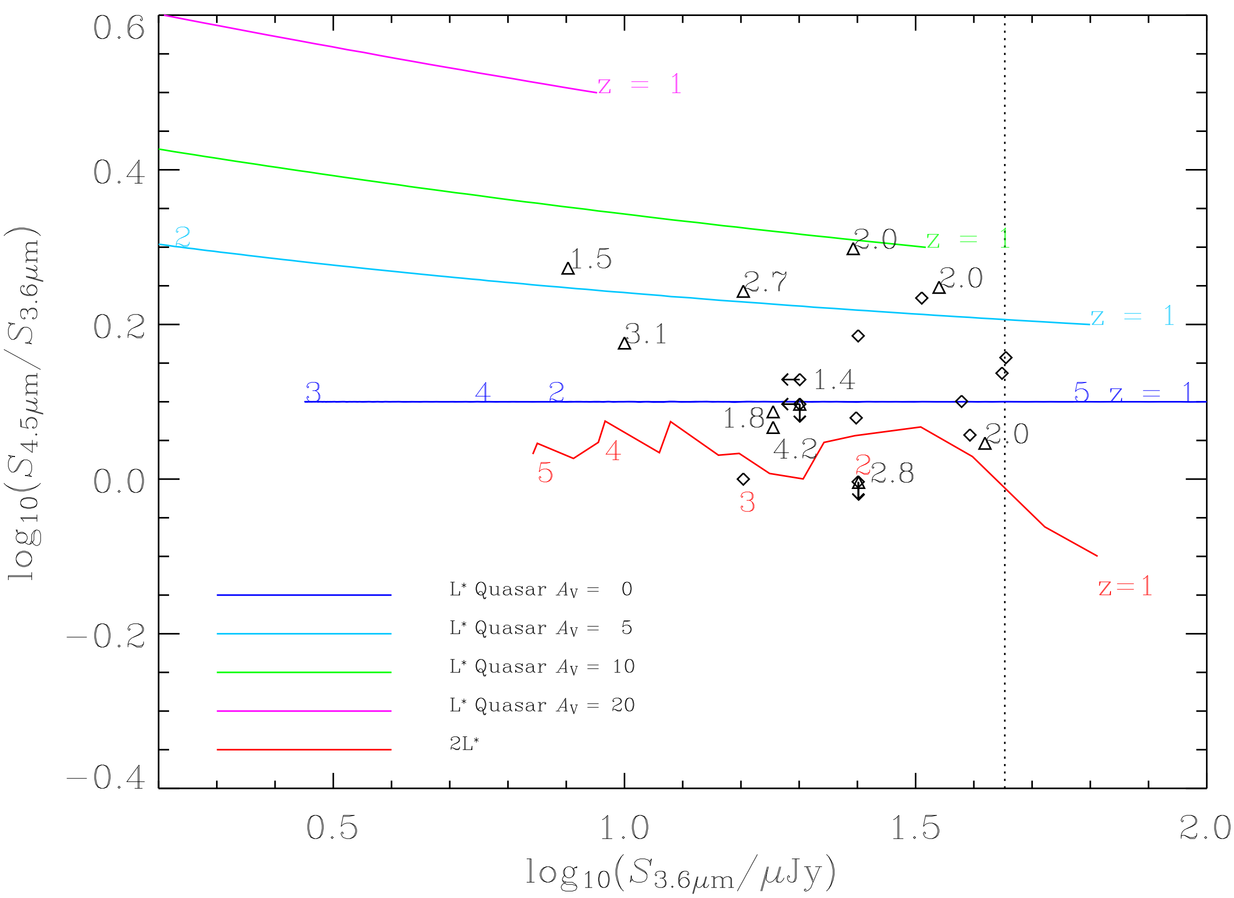

Supplementary FIG. 1. Comparison of photometric and spectroscopic redshifts and possible contamination of the 3.6 μm flux density from obscured quasar light. Log_{10}(3.6 μm flux density $S_{3.6\mu\text{m}}$ / μJy) plotted against $\log_{10}$(3.6 μm flux density $S_{3.6\mu\text{m}}$/ 4.5 μm flux density $S_{4.5\mu\text{m}}$). The dotted line represents the $S_{3.6\mu m} \leq 45\mu$ Jy cut. The symbols have the same meaning as in FIG. 1; the triangles have the spectroscopic redshift plotted next to them. The red track represents the values as a function of z for an elliptical $2L^{*}_{gal}$[6] galaxy evolving passively[26], with the red numbers on the track indicating the redshift. The other lines represent the values for an L^{*}_{quasar} quasar with different amounts of extinction, subject to pure luminosity evolution[15]; again, the coloured numbers on the tracks indicating the redshift. For $A_V \gtrsim 10$ both the 3.6 and 4.5 μm flux densities are dominated by starlight, so the observed flux densities (and their ratio) will be dominated by the host galaxy. However, for $A_V \sim 5$, there will be some contribution from the quasar to both flux densities and the photometric redshift based on the $K - z$ relation, which assumes all the flux density originates in stars, will be slightly underestimated. In addition, for $A_V \sim 5$, the 4.5 μm flux density will have more significant contribution from the quasar than the 3.6 μm flux density, so the ratio will change. This change in ratio can also be caused by a dusty starburst component[20], which will be brighter at longer wavelengths. From this plot it is clear that the photometric redshifts z_{phot}, (represented by the tracks) are in good agreement with the spectroscopic redshifts z_{spec} as the contribution from $A_V \sim 5 - 10$ quasars will only significantly affect $S_{4.5\mu m}$ but not $S_{3.6\mu m}$. We could plausibly be missing a few Type-2 quasars with $z \sim 2$, low A_V and luminous host galaxies: a $z = 2$ Type-2 quasar becomes too bright to be selected if the host galaxy luminosity exceeds $\sim 3.5L^{*}_{gal}$, which is unlikely for a starlight-dominated radio-quiet quasar[6]. If the flux density at 3.6 μm had some additional non-stellar contribution at 3.6 μm for low values of A_V (< 5) then the quasar would not make our selection criteria, and rightly so, as it would not normally be considered a Type-2[4].